The Fe_4S_4 Centers in Ferredoxins Studied through Proton and Carbon Hyperfine Coupling. Sequence-Specific Assignments of Cysteines in Ferredoxins from *Clostridium acidi urici* and *Clostridium pasteurianum*

Ivano Bertini,*,† Francesco Capozzi,‡ Claudio Luchinat,‡ Mario Piccioli,† and Alejandro J. Vila†,§

Contribution from the Department of Chemistry, University of Florence, Florence, Italy, and Institute of Agricultural Chemistry, University of Bologna, Bologna, Italy

Received August 4, 1993®

Abstract: Oxidized ferredoxin from *Clostridium acidi urici*, containing two $[Fe_4S_4]^{2+}$ clusters, has been investigated through ^1H NOESY and TOCSY spectroscopies. The protons of coordinated cysteines have been identified and assigned to each cluster with use of a procedure based on the assignment of two spatially close βCH_2 pairs and on the shift ratios of each βCH_2 proton in oxidized, half-reduced, and reduced forms; each cysteine proton has been then sequence-specifically and stereospecifically assigned by looking for dipolar connectivities with amino acid residues in the vicinity of the cluster. By comparing the present data with the available spectra of the analogous protein from *Clostridium pasteurianum*, the sequence-specific and stereospecific assignments of cysteine protons have been obtained also for the latter protein. The natural abundance ^{13}C signals of the cysteine protons have been also sequence-specifically assigned. By taking advantage of the X-ray structure of a similar protein, the ^1H and ^{13}C hyperfine shifts have been related to the dihedral angle between the iron–sulfur–β-carbon plane and the sulfur–β-carbon–β-proton or sulfur–β-carbon–α-carbon planes. A parametric equation is proposed. The spin delocalization mechanism has been found to be largely dependent on unpaired spin density on the p_z orbital of the sulfur atom. Through EXSY spectroscopy, the proton signals of the $[Fe_4S_4]^+$ clusters in the reduced protein have been assigned. Their temperature dependence is compared with that of the $[Fe_4S_4]^{3+}$ clusters present in oxidized HiPIPs and discussed in terms of the Heisenberg model for the magnetic exchange coupling within the clusters.

Introduction

Ferredoxins containing Fe_4S_4 cores are common electron-transfer proteins.[1-5] They formally contain two Fe^{3+} and two Fe^{2+} ions in the oxidized state ($[Fe_4S_4]^{2+}$ cluster) and three Fe^{2+} and one Fe^{3+} ions in the reduced state ($[Fe_4S_4]^+$ cluster). When oxidized, the ground state of the cluster is $S = 0$. In this state the proteins are EPR silent; the Mössbauer data are consistent with four equivalent iron ions with oxidation number 2.5+.[6-11] Some paramagnetism arises from the population of the excited states.[12] ^1H NMR studies are available on the protein from *Clostridium pasteurianum*, which contains two clusters. These studies have led to assignments of the cysteine βCH_2 protons through deuterium labeling.[13] NOE measurements have related such signals in a pairwise fashion.[14] Finally, NOESY and COSY spectra have permitted the identification of all the βCH_2 and of some αCH cysteine proton signals.[15,16]

When fully reduced, the proteins have a ground state $S = {}^1/_2$ with typical EPR spectra.[17-22] The Mössbauer spectrum is available for the two-cluster protein from *C. pasteurianum*.[7,8] No information on the oxidation state of the iron ions could be obtained owing to the lack of resolution. Magnetic Mössbauer indicates two sets of hyperfine coupling constants between the $S = {}^1/_2$ spin state of the cluster and the ^{57}Fe nuclei, which differ

* Address correspondence to this author at Laboratorio di Chimica Inorganica e Bio, Universita degli Studi di Firenze, Via G. Capponi, 7, 50121 Florence, Italy. Phone 39.55.2757549. Fax 39.55.2757555.

† University of Florence.

‡ University of Bologna.

§ Present address: Catedra de Biofisica, Dto. de Quimica Biologica, Facultad de Ciencias Bioquimicas y Farmaceuticas, Universitad Nacional de Rosario, Suipacha 531, 2000 Rosario, Argentina.

® Abstract published in *Advance ACS Abstracts,* December 1, 1993.

(1) Thompson, A. J. In *Metalloproteins*; Harrison, P., Ed.; Verlag Chemie: Weinheim, FRG, 1985; pp 79.

(2) Berg, J. M.; Holm, R. H. In *Iron-Sulfur Proteins*; Spiro, T. G., Ed.; Wiley-Interscience: New York, 1982; pp 1–66.

(3) Sieker, L. C.; Adman, E. T.; Jensen, L. H. *Nature* **1972**, *235*, 40.

(4) Nagayama, K.; Ohmori, D.; Imai, Y.; Oshima, T. In *Iron-Sulfur Protein Research*; Matsubara, H., Ed.; Springer-Verlag: Berlin, 1986; pp 125–138.

(5) Cammack, R. In *Advances in Inorganic Chemistry. Vol. 38: Iron Sulfur Proteins*; Cammack, R., Sykes, A. G., Eds.; Academic Press: San Diego, CA, 1992; pp 281–322.

(6) Moss, T. H.; Bearden, A. J.; Bartsch, R. G.; Cusanovich, M. A.; San Pietro, A. *Biochemistry* **1968**, *7*, 1591.

(7) Thompson, C. L.; Johnson, C. E.; Dickson, D. P. E.; Cammack, R.; Hall, D. O.; Weser, U.; Rao, K. K. *Biochem. J.* **1974**, *139*, 97.

(8) Gersonde, K.; Schlaak, H.-E.; Breitenbach, M.; Parak, F.; Eicher, H.; Zgorzalla, W.; Kalvius, M. G.; Mayer, A. *Eur. J. Biochem.* **1974**, *43*, 307.

(9) Mullinger, R. N.; Cammack, R.; Rao, K. K.; Hall, D. O.; Dickson, D. P. E.; Johnson, C. E.; Rush, J. D.; Simonopulos, A. *Biochem. J.* **1975**, *151*, 75.

(10) Dickson, D. P. E.; Johnson, C. E.; Middleton, P.; Rush, J. D.; Cammack, R.; Hall, D. O.; Mullinger, R. N.; Rao, K. K. *J. Phys., Colloq.* **1976**, *37*, C6–171.

(11) Middleton, P.; Dickson, D. P. E.; Johnson, C. E.; Rush, J. D. *Eur. J. Biochem.* **1978**, *88*, 135.

(12) Poe, M.; Phillips, W. D.; McDonald, C. C.; Lovenberg, W. *Proc. Natl. Acad. Sci. U.S.A.* **1970**, *65*, 797.

(13) Packer, E. L.; Sweeney, W. V.; Rabinowitz, J. C.; Sternlicht, H.; Shaw, E. N. *J. Biol. Chem.* **1977**, *252*, 2245.

(14) Bertini, I.; Briganti, F.; Luchinat, C.; Scozzafava, A. *Inorg. Chem.* **1990**, *29*, 1874.

(15) Bertini, I.; Briganti, F.; Luchinat, C.; Messori, L.; Monnanni, R.; Scozzafava, A.; Vallini, G. *FEBS Lett.* **1991**, *289*, 253.

(16) Busse, S. C.; La Mar, G. N.; Howard, J. B. *J. Biol. Chem.* **1991**, *266*, 23714.

(17) Mathews, R.; Charlton, S.; Sands, R. H.; Palmer, G. *J. Biol. Chem.* **1974**, *249*, 4326.

(18) Munck, E.; Huynh, B. H. In *ESR and NMR of Paramagnetic Species in Biological and Related Systems*; Bertini, I., Drago, R. S., Eds.; D. Reidel: Dordrecht, 1979; Chapter 12.

(19) Holm, B. O.; Evans, M. C. W. *Nature* **1969**, *223*, 1342.

(20) Anderson, R. E.; Anger, G.; Petersson, L.; Ehrenberg, A.; Cammack, R.; Hall, D. O.; Mullinger, R.; Rao, K. K. *Biochim. Biophys. Acta* **1975**, *376*, 63.

(21) Stombaugh, N. A.; Burris, R. H.; Orme-Johnson, W. H. *J. Biol. Chem.* **1973**, *248*, 7951.

(22) Yoch, D. C.; Carithers, R. P.; Arnon, D. I. *J. Biol. Chem.* **1977**, *252*, 7453.

0002-7863/94/1516-0651$04.50/0

also in sign.[7] Mössbauer data are also available for the ferredoxin from *Bacillus stearothermophilus*, which contains a single cluster.[9-11] In this case, two pairs of iron ions were observed. The hyperfine coupling value with the ^{57}Fe nuclei could be consistent with the mixed-valence pair ($Fe^{2.5+}$ ions) having a local subspin larger than that of the Fe^{2+} ions.[11] This situation can be reproduced with a Heisenberg Hamiltonian under a variety of conditions.[23,24]

The ^1H NMR spectra of all reduced proteins show downfield shifted signals. The temperature dependencies of the shifts invariably show some hyperfine shifted signals having an anti-Curie behavior (*i.e.*, the shifts increase with increasing temperature).[12-14,25-29] In ferredoxin from *C. pasteurianum*, through EXSY spectroscopy as many as six or seven out of eight βCH_2 signals per cluster could be identified.[24]

In the case of paramagnetic metalloproteins, the protons close to the metal clusters are easily recognizable because they have short T_1 and T_2 values.[30] If we are able to reveal connectivities between such fast-relaxing protons and protons in the diamagnetic region and the latter are recognized to belong, from COSY and TOCSY spectra, to a certain amino acid residue, then by looking at the X-ray structure or at any reliable model it is possible to perform the stereospecific, sequence-specific assignment of the protons involved in the connectivity patterns.[31-35] This approach has been successful for many metalloproteins, including cobalt(II)-substituted carbonic anhydrase,[36,37] copper(II), cobalt(II) superoxide dismutase,[38-41] a number of heme proteins,[42-69] and as many as six high-potential iron–sulfur proteins.[31-35,70] In many cases, the assignment is helped by the presence of nearby residues with unique connectivity patterns, especially aromatic residues. Although low-potential iron–sulfur proteins have been heavily investigated by NMR for many years, no stereospecific, sequence-specific assignment is available for any of them. The main difficulties encountered in such systems are (i) the absence of aromatic residues in the neighborhood of the cluster and (ii) the close similarity between the two clusters that makes difficult even the cluster-specific assignment. Recently, the latter has been successfully performed on the *C. pasteurianum* ferredoxin.[24] A tentative sequence-specific assignment of the cysteine proton signals was proposed[16] under the assumption that the hyperfine shifts of the βCH_2 protons have a dependence on the Fe–S–C–H dihedral angle of the type $\delta = a + b\cos^2\theta$. This simplified Karplus[71,72] relationship was originally proposed for aliphatic amines coordinated to Ni^{2+} [73-75] but may not be adequate in iron–sulfur systems.[32,33,76]

In this paper we report the first stereospecific, sequence-specific assignment of cysteine protons in an (Fe_4S_4) or $(Fe_4S_4)_2$ ferredoxin. We have chosen the $(Fe_4S_4)_2$ ferredoxin from *Clostridium acidi urici* because of its relatively high yield and because its ^1H NMR spectra, already reported, are of high quality. We have found that in the latter protein, which is very similar to the *C. pasteurianum* protein, a few key connectivities are more readily observed. Moreover, for the first time, we have detected the ^{13}C signals of the cysteines through heteronuclear multiple quantum coherence (HMQC) experiments on samples not isotopically enriched. Since the spectra of the protein from *C. pasteurianum* are quite similar to those obtained in the present system,[13-16,24,27-29] the sequence-specific assignment of the signals of the *C. pasteurianum* ferredoxin is also achieved. The latter is different from the tentative assignment based on the dihedral angles.[16] Indeed, by analyzing in detail the angular dependence of the hyperfine coupling not only for β-cysteine protons, but also for α-carbons, we could establish a new functional form for the angular dependence, essentially opposite to the commonly used one.

(23) Jordanov, J.; Roth, E. K. H.; Fries, P. H.; Noodleman, L. *Inorg. Chem.* **1990**, *29*, 4288.
(24) Bertini, I.; Briganti, F.; Luchinat, C.; Messori, L.; Monnanni, R.; Scozzafava, A.; Vallini, G. *Eur. J. Biochem.* **1992**, *204*, 831.
(25) Nagayama, K.; Ozaki, Y.; Kyogoku, Y.; Hase, T.; Matsubara, H. *J. Biochem.* **1983**, *94*, 893.
(26) Phillips, W. D.; McDonald, C. C.; Stombaugh, N. A.; Orme-Johnson, W. H. *Proc. Natl. Acad. Sci. U.S.A.* **1974**, *71*, 140.
(27) Phillips, W. D.; Poe, M. In *Iron–Sulfur Proteins*; Lovenberg, W., Ed.; Academic: New York, 1977; Vol. 3, Chapter 7.
(28) Phillips, W. D. In *NMR of Paramagnetic Molecules*; La Mar, G. N., Horrocks, W. D., Jr., Holm, R. H., Eds.; Academic: New York, 1973; Chapter 11.
(29) Gaillard, J.; Moulis, J.-M.; Meyer, J. *Inorg. Chem.* **1987**, *26*, 320.
(30) Banci, L.; Bertini, I.; Luchinat, C. *Nuclear and Electron Relaxation. The Magnetic Nucleus-Unpaired Electron Coupling in Solution*; VCH: Weinheim, 1991.
(31) Bertini, I.; Capozzi, F.; Luchinat, C.; Piccioli, M.; Vicens Oliver, M. *Inorg. Chim. Acta* **1992**, *198–200*, 483.
(32) Bertini, I.; Capozzi, F.; Ciurli, S.; Luchinat, C.; Messori, L.; Piccioli, M. *J. Am. Chem. Soc.* **1992**, *114*, 3332.
(33) Bertini, I.; Capozzi, F.; Luchinat, C.; Piccioli, M. *Eur. J. Biochem.* **1993**, *212*, 69.
(34) Banci, L.; Bertini, I.; Ciurli, S.; Ferretti, S.; Luchinat, C.; Piccioli, M. *Biochemistry*, in press.
(35) Banci, L.; Bertini, I.; Capozzi, F.; Carloni, P.; Ciurli, S.; Luchinat, C.; Piccioli, M. *J. Am. Chem. Soc.* **1993**, *115*, 3431.
(36) Banci, L.; Dugad, L. B.; La Mar, G. N.; Keating, K. A.; Luchinat, C.; Pierattelli, R. *Biophys. J.* **1992**, *63*, 530.
(37) Bertini, I.; Luchinat, C.; Pierattelli, R.; Vila, A. J. *Eur. J. Biochem.* **1992**, *208*, 607.
(38) Banci, L.; Bencini, A.; Bertini, I.; Luchinat, C.; Piccioli, M. *Inorg. Chem.* **1990**, *29*, 4867.
(39) Bertini, I.; Luchinat, C.; Piccioli, M.; Vicens Oliver, M.; Viezzoli, M. S. *Eur. J. Biophys.* **1991**, *20*, 269.
(40) Bertini, I.; Luchinat, C.; Ming, L. J.; Piccioli, M.; Sola, M.; Valentine, J. S. *Inorg. Chem.* **1992**, *31*, 4433.
(41) Banci, L.; Bertini, I.; Luchinat, C.; Piccioli, M.; Scozzafava, A. *Gazz. Chim. Ital.* **1993**, *123*, 95.
(42) Thanabal, V.; La Mar, G. N. *Biochemistry* **1989**, *28*, 7038.
(43) Veitch, N. C.; Williams, R. J. P. *Eur. J. Biochem.* **1990**, *189*, 351.
(44) Emerson, S. D.; La Mar, G. N. *Biochemistry* **1990**, *29*, 1545.
(45) Berry, M. J.; George, S. J.; Thomson, A. J.; Santos, H.; Turner, D. L. *Biochem. J.* **1990**, *270*, 413.
(46) de Ropp, J. S; La Mar, G. N. *J. Am. Chem. Soc.* **1991**, *113*, 4348.
(47) Yamamoto, Y.; Iwafune, K.; Nanai, N.; Osawa, A.; Chujo, R.; Suzuki, T. *Eur. J. Biochem.* **1991**, *198*, 299.
(48) Yamamoto, Y.; Chujo, R.; Suzuki, T. *Eur. J. Biochem.* **1991**, *198*, 285.
(49) Satterlee, J. D.; Erman, J. E. *Biochemistry* **1991**, *30*, 4398.
(50) Satterlee, J. D.; Russell, D. J.; Erman, J. E. *Biochemistry* **1991**, *30*, 9072.
(51) Lee, K. B.; Jun, E.; La Mar, G. N.; Rezzano, I. N.; Pandey, R. K.; Smith, K. M.; Walker, F. A.; Buttlaire, D. H. *J. Am. Chem. Soc.* **1991**, *113*, 3576.
(52) de Ropp, J. S.; La Mar, G. N.; Wariishi, H.; Gold, M. H. *J. Biol. Chem.* **1991**, *266*, 15001.
(53) Banci, L.; Bertini, I.; Turano, P.; Tien, M.; Kirk, T. K. *Proc. Natl. Acad. Sci. U.S.A.* **1991**, *88*, 6956.
(54) La Mar, G. N.; Hernández, G.; de Ropp, J. S *Biochemistry* **1992**, *31*, 9158.
(55) Veitch, N. C.; Williams, R. J. P.; Bray, R. C.; Burke, J. F.; Sanders, S. A.; Thornley, R. N. F.; Smith, A. T. *Eur. J. Biochem.* **1992**, *207*, 521.
(56) Rajarathnam, K.; La Mar, G. N.; Chiu, M. L.; Sligar, S. G. *J. Am. Chem. Soc.* **1992**, *114*, 9048.
(57) Yamamoto, Y.; Iwafune, K.; Chujo, R.; Inoue, Y.; Imai, K.; Suzuki, T. *J. Biochem.* **1992**, *112*, 414.
(58) Moench, S.; Chroni, S.; Lou, B. S.; Erman, J. E.; Satterlee, J. D. *Biochemistry* **1992**, *31*, 3661.
(59) Dugad, L. B.; Wang, X.; Wang, C.-C.; Lukat, G. S.; Goff, H. M. *Biochemistry* **1992**, *31*, 1651.
(60) Santos, H.; Turner, D. L. *Eur. J. Biochem.* **1992**, *206*, 721.
(61) Costa, H. S.; Santos, H.; Turner, D. L.; Xavier, A. V. *Eur. J. Biochem.* **1992**, *208*, 427.
(62) Salguerio, C. A.; Turner, D. L.; Santos, H.; LeGall, J.; Xavier, A. V. *FEBS Lett.* **1992**, *314*, 155.
(63) Sola, M.; Cowan, J. A. *Inorg. Chim. Acta* **1992**, *202*, 241.
(64) Saraiva, L. M.; Denariaz, G.; Liu, M.-Y.; Payne, W. J.; LeGall, J.; Moura, I. *Eur. J. Biochem.* **1992**, *204*, 1131.
(65) Dugad, L. B.; Goff, H. M. *Biochim. Biophys. Acta* **1992**, *1122*, 63.
(66) Bertini, I.; Gori, G.; Luchinat, C.; Vila, A. J. *Biochemistry* **1993**, *32*, 776.
(67) Turner, D. L. *Eur. J. Biochem.* **1993**, *211*, 563.
(68) Turner, D. L.; Williams, R. J. P. *Eur. J. Biochem.* **1993**, *211*, 555.
(69) Banci, L.; Bertini, I.; Bini, T.; Tien, M.; Turano, P. *Biochemistry* **1993**, *32*, 5825.
(70) Bertini, I.; Gaudemer, A.; Luchinat, C.; Piccioli, M. *Biochemistry*, in press.
(71) Karplus, M. *J. Chem. Phys.* **1959**, *30*, 11.
(72) Karplus, M. *J. Am. Chem. Soc.* **1963**, *85*, 2870.
(73) Fitzgerald, R. J.; Drago, R. S. *J. Am. Chem. Soc.* **1968**, *90*, 2523.
(74) Ho, F. F.-L.; Reilley, C. N. *Anal. Chem.* **1969**, *41*, 1835.
(75) Pratt, L.; Smith, B. B. *Trans. Faraday Soc.* **1968**, *65*, 915.
(76) Mouesca, J. M.; Rius, G.; Lamotte, B. *J. Am. Chem. Soc.* **1993**, *115*, 4714.

Finally, the temperature dependence of the shifts allowed us to make some progress in understanding the electronic structure of the reduced form of the protein. It turned out that the magnetic coupling in the latter chromophore is much less readily accounted for with the simple coupling schemes which were successful for oxidized HiPIPs.[77-79]

Experimental Part

Protein Preparation. *Clostridium acidi urici* (DSM 604[80]) was grown in a medium containing uric acid as carbon source.[81] The procedure used to purify the protein is a modification of a previously described method.[82] Wet cells (150 g) obtained from 20 batches of 10-L cultures were suspended in 250 mL of 0.05 M potassium phosphate buffer at pH = 7.8 and disrupted with a French press operating at 35 000 psi. After centrifugation of the suspension at 12 000*g* for 30 min and 40 000*g* for 1 h, the supernatants were pooled and loaded onto a column of Whatman DE-52 DEAE-cellulose equilibrated with distilled water. The column was washed with water, and then a linear gradient from 0.1 to 0.7 M NaCl was applied. The ferredoxin was eluted as a dark green band. The fractions containing ferredoxins were pooled, diluted 4-fold with water, and applied again onto a column of DE-52 equilibrated with 0.15 M Tris·HCl, pH = 7.4. The ferredoxin was eluted with a linear gradient from 0.07 to 0.27 M NaCl in 0.15 M Tris·HCl, pH = 7.4. The fractions containing ferredoxin were pooled and concentrated to 5 mL by loading them onto a small DE-52 column and eluting the protein with 0.5 M NaCl in 0.15 M Tris·HCl, pH = 7.4. The last purification step, consisting of a gel filtration through Sephadex G-75, gave 70 mg of ferredoxin with an absorbance ratio A_{390}/A_{280} of 0.78.

NMR Measurements. Purified protein solutions were repeatedly exchanged with D_2O (99.9%) solutions containing 50 mM phosphate buffer at pH* = 7.8. Sample concentrations were about 20 mM for all the experiments performed on the fully oxidized protein. The experiments on the partially reduced protein were performed using a 2 mM protein concentration. Sample volumes were 0.500 mL. All the experiments were performed, at temperatures ranging from 282 to 300 K, on a Bruker AMX 600 operating at the magnetic field of 14 T. A 5-mm ^1H probe was used. The spectra were calibrated by referencing to the residual HDO signal, assigned a 4.78-ppm shift at 298 K. COSY experiments[83] were performed in magnitude mode. From 200 to 800 increments in the F1 dimension were collected by recording 1024–2048 points for each FID in the F2 dimension over a spectral window of about 15 kHz. Recycle delays from 100 to 800 ms were used. NOESY[84] and TOCSY[85] experiments were recorded in phase-sensitive TPPI mode. When the NOESY spectra were performed to obtain information involving hyperfine shifted signals, from 250 to 800 increments in the F1 dimension were collected using 1024 data points in the F2 domain. Mixing times from 5 to 30 ms and a relaxation delay of about 120 ms were used. In order to detect NOESY connectivities involving signals not affected by hyperfine interaction, 2048 × 1024-data point matrices were acquired, over 7500 Hz of spectral width, using mixing times and relaxation delays of 30 and 370 ms, respectively. TOCSY experiments were performed over a 7500-Hz spectral region. 2048 × 1024-data point matrices were acquired using 64 scans for each experiment. Spin lock times of 40 ms and relaxation delays of 400 ms were used. The EXSY experiments at variable temperatures were recorded using the same pulse sequence used for NOESY experiments.[86] 1024 × 512-data point matrices were acquired using mixing times and relaxation delays of 5 and 55 ms, respectively. The EXSY experiments have been recorded over a 72-kHz spectral region. A high-power 5-mm probe (Bruker) capable of delivering a 90° proton pulse as short as 4.3 μs was used to record the spectra. ^1H–^{13}C heteronuclear correlation experiments were performed using an 18-kHz spectral width in the F2 dimension (^1H) and a 60-kHz spectral width in the F1 dimension (^{13}C). The four-pulse ($90°_{^1H}$–d–$90°_{^{15}N}$–$t_{1/2}$–$180°_{^1H}$–$t_{1/2}$–$90°_{^{15}N}$–d–AQ) HMQC pulse sequence[87] was used. The experiments were performed in magnitude mode. An inverse detection 5-mm probe (Bruker) was used for the heterocorrelated experiments. About 1024 × 174-data points matrices were acquired, using 1024 scans for each FID. Refocusing and recycle delay were 1.5 and 15 ms, respectively. Data processing was performed either on the standard software package provided by Bruker or on a home-made program for NMR data processing, based on the IDL software package (CreaSo, Gilching, Ger) and run on an IBM RISC 6000/550.

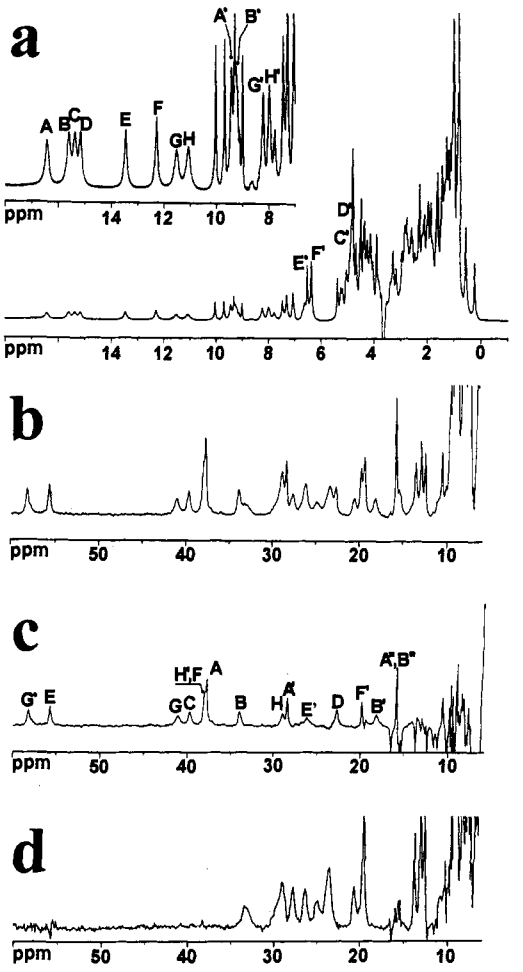

Figure 1. 600-MHz ^1H NMR spectra of ferredoxin from *C. acidi urici*, recorded at 298 K. (a) Oxidized species **1**, (b) partially reduced sample, (c) reduced species **4**, (d) intermediate species **2** + **3**. Spectrum d was obtained by recording the ^1H NMR spectrum of a 90% oxidized, 10% partially reduced ferredoxin and by subtracting from the recorded spectrum the spectrum of the fully oxidized species (a) properly scaled. Spectrum c was obtained by recording the spectrum of a ferredoxin sample containing both partially reduced and fully reduced ferredoxin and by subtracting from the recorded spectrum that of the intermediate species (d). Signal labeling is reported according to Table 1. The identification of signal E′ in the fully reduced derivative is tentatively proposed only on the basis of the difference spectrum reported in Figure 1c, in which a broad resonance, not assigned through the magnetization-transfer experiment, is observed at a chemical shift value consistent with that expected for signal E′ in the reduced form on the basis of the observed shift in the oxidized and partially reduced forms. For all the other signals, direct evidence for the correspondence between oxidized and reduced forms has been obtained through saturation transfer experiments (see Figure 3).

Results and Discussion

Pairwise Assignment. The 600-MHz ^1H NMR spectrum of oxidized ferredoxin from *C. acidi urici* is reported in Figure 1a.

(77) Noodleman, L. *Inorg. Chem.* **1988**, *27*, 3677.
(78) Blondin, G.; Girerd, J.-J. *Chem. Rev.* **1990**, *90*, 1359.
(79) Banci, L.; Bertini, I.; Briganti, F.; Luchinat, C.; Scozzafava, A.; Vicens Oliver, M. *Inorg. Chem.* **1991**, *30*, 4517.
(80) DSM: Deutsche Samlung von Microorganism.
(81) Rabinowitz, J. C. *Methods Enzymol.* **1963**, *6*, 703.
(82) Rabinowitz, J. C. *Methods Enzymol.* **1972**, *24*, 431.
(83) Bax, A.; Freeman, R.; Morris, G. *J. Magn. Reson.* **1981**, *42*, 164.
(84) Macura, S.; Ernst, R. R. *Mol. Phys.* **1980**, *41*, 95.
(85) Bax, A.; Davis, D. G. *J. Magn. Reson.* **1985**, *63*, 207.
(86) Santos, H.; Turner, D. L.; Xavier, A. V.; LeGall, J. *J. Magn. Reson.* **1985**, *55*, 177.
(87) (a) Bax, A.; Griffey, R. H.; Hawkins, B. L. *J. Am. Chem. Soc.* **1983**, *105*, 7188. (b) Bax, A.; Griffey, R. H.; Hawkins, B. L. *J. Magn. Reson.* **1983**, *55*, 301.

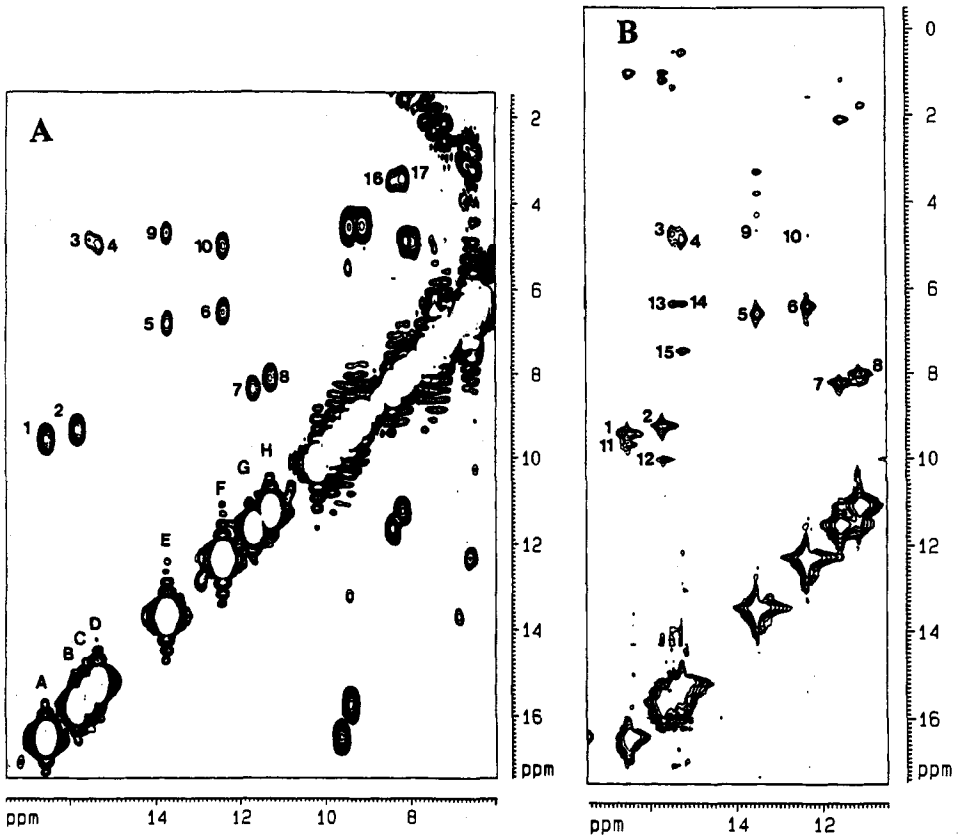

Figure 2. (A) COSY and (B) NOESY spectra of oxidized ferredoxins from *C. acidi urici*. Connectivities labeled 1–8 refer to the β–β connectivities observed in both COSY (A) and NOESY (B) spectra for all the eight cysteines bound to the clusters. Connectivities labeled 9–17 refer to the observed β–α connectivities. Connectivities 9 and 10 were observed in both COSY and NOESY experiments; connectivities 11–15 were observed only in NOESY (B) and connectivities 16,17 only in COSY spectra. The reported experiments were optimized for the detection of connectivities between cysteine protons.

Except for the better resolution due to the higher field, the spectrum is in agreement with those previously reported.[13] Eight signals are observed outside the diamagnetic envelope, which are labeled from A to H. Fast relaxation rates and anti-Curie temperature dependence indicate that signals A–H belong to protons of cluster-coordinated cysteines.

COSY and NOESY experiments, reported in Figure 2, show scalar[88] and dipolar connectivities arising from such resonances. Each of the eight most shifted signals gives one (signals A, B, C, D, G, H) or two (E, F) connectivities in the COSY spectrum (Figure 2A, connectivities 1–10) with signals spread in the 10–4-ppm region. Repetition of COSY experiments at different temperatures shows that all the signals in the diamagnetic region which are involved in connectivities 1–10 in Figure 2A have anti-Curie temperature dependence and account for all the βCH_2 pairs of cluster-coordinated cysteines plus two α-β connectivities (connectivities 9 and 10). Of course, the NOESY experiments (Figure 2B) confirm the pairwise assignment. The pairwise assignment of all cysteine βCH_2 protons is listed in Table 1, columns 1–3.

Besides their geminal partners, labeled A′–H′, each of the hyperfine shifted signals A–H experiences other strong connectivities in the NOESY experiments. Among these, cross peaks labeled 9–15 in Figure 2B involve signals which experience anti-Curie temperature dependence and are thus assigned to the αCH protons of cluster-coordinated residues. Two of them (connectivities 9 and 10) are observed also in the COSY experiment. The αCH protons of cysteines VII and VIII (whose βCH_2 protons correspond to signals G,G′ and H,H′, respectively) are assigned owing to the scalar connectivities from signals G′ and H′ (cross peaks 16 and 17). The temperature dependence of cross peaks 16 and 17 is consistent with their assignment as α-β connectivities of cysteines VII and VIII.

Signals C and D display NOESY cross peaks (13,14) with the same Cys αCH signal at 6.36 ppm. From now on, we need a structural model to proceed with the assignment. We take the X-ray structure of the *Peptococcus aerogenes* ferredoxin as our model.[89,90] The homology between the two proteins is 68% and reaches 87% in the proximity of the cluster.[91] Therefore the structure of the ferredoxin from *P. aerogenes* is a good model for the ferredoxins discussed here, at least as far as the neighborhood of the cluster is concerned. Inspection of the X-ray structure reveals that only in the case of two cysteines, namely Cys 42 (corresponding to Cys 43 in *C. acidi urici* and *C. pasteurianum* ferredoxins) and Cys 14, is there the possible occurrence of an interresidue dipolar connectivity involving two of the cluster-coordinated cysteines. Indeed, Cys 42 Hα is at 2.7 Å from Cys 14 Hβ_1. This unique structural feature is by itself sufficient to stereospecifically assign signals C,C′ and D,D′ as the βCH_2 protons of Cys 43 and Cys 14, respectively. We note here that this same connectivity has been previously observed as a very weak cross peak in *C. pasteurianum* ferredoxin but not utilized for assignment.[16] Slight structural inequivalences between *C. pasteurianum* ferredoxin and *C. acidi urici* ferredoxin can easily explain the more intense NOESY cross peak observed in the present case.

Cluster-Specific Assignment. The cluster-specific assignment was performed following the same strategy used for *C. pasteur-*

(88) It has been recently shown that COSY cross peaks observed in paramagnetic metalloproteins may not arise from scalar coupling but from cross-correlation effects between dipolar proton–proton relaxation and Curie relaxation [Bertini, I.; Luchinat, C.; Tarchi, D. *Chem. Phys. Lett.* **1993**, 203, 445–449]. In the present system having rather small molecular weight and $S = 1/2$, Curie relaxation is estimated to be nonimportant and COSY cross peaks are due to scalar couplings.

(89) Adman, E. T.; Sieker, L. C.; Jensen, L. H. *J. Biol. Chem.* **1973**, *248*, 3987.

(90) Adman, E. T.; Sieker, L. C.; Jensen, L. H. *J. Biol. Chem.* **1976**, *251*, 3801.

(91) KrishnaMurthy, H. M.; Hendrickson, W. A.; Orme-Johnson, W. H.; Merritt, E. A.; Phizackerley, R. P. *J. Biol. Chem.* **1988**, *263*, 18430.

Table 1. Sequence-Specific Assignment of the ^{1}H NMR Signals of Ferredoxin from *C. acidi urici* at 293 K, pH 7.8, and Assignment of Ferredoxin from *C. pasteurianum* Deduced from the Present Data

		C. acidi urici δ (ppm)			assignment[a]		*C. pasteurianum*[b] δ (ppm)			temperature dependence of
signal	cysteine	oxid[c]	int[c]	red[c]	cluster-specific	sequence-specific	oxid	int	red	shifts in reduced species
A	Cys I Hβ	16.3	27.6	37.7		Cys 40 $H\beta_2$	17.2	31.4	38.8	
A′	Cys I Hβ	9.5	19.0	27.7	cluster II	Cys 40 $H\beta_1$	9.3	24.5	33.3	anti-Curie
A″	Cys I Hα	9.7	13.0	15.7		Cys 40 Hα				
B	Cys II Hβ	15.4	22.7	32.7		Cys 11 $H\beta_2$	15.7	21.6	33.7	
B′	Cys II Hβ	9.2	13.0	18.5	cluster I	Cys 11 $H\beta_1$	9.4	12.7	20.3	anti-Curie
B″	Cys II Hα	10.0	12.4	15.5		Cys 11 Hα				
C	Cys III Hβ	15.2	29.1	39.5		Cys 43 $H\beta_1$	16.1	41.5	60.2	
C′	Cys III Hβ	4.8	13.0	18.5	cluster II	Cys 43 $H\beta_2$	5.1			Curie
C″	Cys III Hα	6.3				Cys 43 Hα				
D	Cys IV Hβ	15.0	19.8	23.9		Cys 14 $H\beta_1$	14.8	18.9	25.8	
D′	Cys IV Hβ	4.8			cluster I	Cys 14 $H\beta_2$	4.9			Curie
D″	Cys IV Hα	7.4				Cys 14 Hα				
E	Cys V Hβ	13.4	32.0	55.9		Cys 47 $H\beta_2$	13.5	27.7	57.0	
E′	Cys V Hβ	6.5	14.8	26.0[d]	cluster I	Cys 47 $H\beta_1$	6.9	31.4	26.9	anti-Curie
E″	Cys V Hα	4.7				Cys 47 Hα				
F	Cys VI Hβ	12.2	26.2	38.2		Cys 18 $H\beta_2$	12.3	22.4	25.6	
F′	Cys VI Hβ	6.4	13.0	22.5	cluster II	Cys 18 $H\beta_1$	6.1			anti-Curie
F″	Cys VI Hα	5.0				Cys 18 Hα				
G	Cys VII Hβ	11.4	25.1	41.5		Cys 8 $H\beta_1$	11.9	23.1	40.7	
G′	Cys VII Hβ	8.2	29.8	56.5	cluster I	Cys 8 $H\beta_2$	8.9	26.1	54.6	Curie
G″	Cys VII Hα	3.5				Cys 8 Hα				
H	Cys VIII Hβ	11.1	20.9	29.3		Cys 37 $H\beta_1$	11.1	18.3	22.0	
H′	Cys VIII Hβ	7.9	24.0	38.2	cluster II	Cys 37 $H\beta_2$	7.9	20.9	28.2	Curie
H″	Cys VIII Hα	3.4				Cys 37 Hα				

[a] The assignments hold for both *C. pasteurianum* and *C. acidi urici* ferredoxins. [b] The sequence-specific, stereospecific assignment of cysteine signals of ferredoxin from *C. pasteurianum* is based on the data reported in refs 15 and 24 and on the similarities between the two proteins (see text). [c] Oxid, oxidized; int, interresidue; red, reduced. [d] Tentative assignment on the basis of the 1D spectra.

Scheme 1

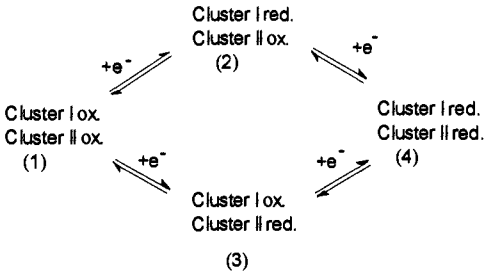

ianum ferredoxin.[24] Addition of small amounts of solid sodium dithionite causes a partial reduction of the oxidized protein. Figure 1b reports the ^{1}H NMR spectrum of a partially reduced derivative. As already observed,[24,92] a partial reduction gives rise to three different species on the basis of Scheme 1. The two partially reduced species **2** and **3** are in fast exchange on the NMR time scale, while the exchange rates between the fully oxidized (**1**) and the two mixed species as well as between the two mixed and the fully reduced (**4**) species are slow. Hence, NMR spectra of a partially reduced sample permit the detection of three different species, the fully reduced species, the intermediate species constituted by species **2** and **3** in fast exchange, and the oxidized species.

As it can be observed from Figure 1c, the signals of the reduced species are rather broad and spread over a large interval of chemical shifts. Rather than relying on the expectedly weak NOESY and COSY cross peaks in the 2D spectra of the reduced form, the assignment of the signals can be more easily performed through EXSY from the oxidized species, as EXSY cross peaks in these systems are known to be very strong.[15]

Figure 3 reports an EXSY experiment performed at 293 K on a partially reduced sample. For 14 out of 16 βCH_2 signals and for two of the eight αCH signals it has been possible to detect the magnetization transfer from the oxidized to the mixed species and then (with a single exception) from the mixed to the fully reduced species. The chemical shifts and the assignments established on the above basis are reported in Table 1, columns 4 and 5.

The chemical shift values of Table 1 allow us to perform the cluster-specific assignment of the eight cysteine residues, which are labeled I–VIII. As previously noted,[92] the two Fe_4S_4 clusters differ slightly in redox potential. Accordingly, species **2** and **3** of Scheme 1 will differently contribute to the mixed species detected through NMR.[24,92] The signals of the four cysteines bound to the more reducible cluster will display a chemical shift, shown in the spectrum of Figure 1d, higher than the average between the shifts in the spectra of Figures 1a and 1c. Of course, the four cysteines bound to the cluster characterized by the smaller reduction potential will experience an opposite behavior. In such a way, Cys I, Cys VI, and Cys VIII are assigned to the more reducible cluster, while Cys II, Cys V, and Cys VII are assigned to the less reducible cluster. Cys III and Cys IV show an anomalous trend. They are already assigned to Cys 43 and Cys 14, respectively. In both cases the cysteine βCH_2 signals in the one-electron-reduced species experience a chemical shift slightly larger (0.5–1.0 ppm) with respect to what is expected on the basis of the above reasoning. This effect might be due to the fact that the two clusters have the closest contact in correspondence of Cys 14 and Cys 43. Therefore, each of them may be influenced by the proximity of the other cluster. Cys III (Cys 43) is assigned to the more reducible cluster because the shifts are more downfield with respect to the average between the fully oxidized and the fully reduced species. The cluster-specific assignment is summarized in Table 1, column 6.

Sequence-Specific Assignment. The NOESY experiments involving hyperfine shifted signals allow us to detect dipolar connectivities from hyperfine coupled signals of cysteine βCH_2s to protons belonging to other residues close in space but not coupled to the unpaired electrons. NOESY and TOCSY experiments in

(92) Packer, E. L.; Sternlicht, H.; Lode, E. T.; Rabinowitz, J. C. *J. Biol. Chem.* **1975**, *250*, 2062.

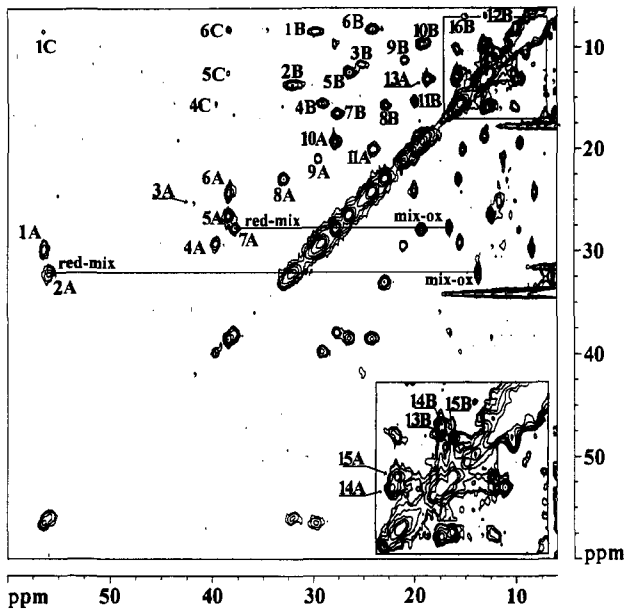

Figure 3. 600-MHz, 293 K EXSY spectrum of *C. acidi urici* ferredoxin. Connectivities between signals of the oxidized and intermediate species and between signals of the intermediate and reduced species are observed. Cross peaks labeled A refer to connectivities between the fully reduced and the intermediate species, those labeled B to connectivities between the mixed and the fully oxidized species. For many signals, it has been also possible to observe cross peaks between the fully reduced and the fully oxidized species. For the sake of clarity, only some of such cross peaks are identified in the figure and labeled C. Each cross peak is assigned to a cysteine proton, according to signal labeling reported in Table 1: 1-G′, 2-E, 3-G, 4-C, 5-F, 6-H′, 7-A, 8-B, 9-H, 10-A′, 11-D, 12-F′, 13-B′, 14-A″, 15-B″, 16-E′. Cross peak 12A (signal F′) is at the limit of detection, and it is not observable in the figure, although it has been identified at different temperatures. The connectivity between partially and fully reduced species of signal E′ (which should correspond to cross peak 16A) has not been observed. The identification of signal E′ in the fully reduced form is only tentative (see caption to Figure 1), as it has not been performed on the ground of EXSY data. EXSY experiments have been performed at the following temperatures: 282, 287, 293 (reported in figure), and 300 K. All cross peaks labeled in the figure have been observed in all EXSY experiments at different temperatures.

the diamagnetic region, reported in Figure 4, make it possible, at least in some cases, to assign some of the proton signals that are dipole–dipole coupled to cysteine protons. In this way the sequence-specific assignment of each of the eight cysteine residues could be achieved. The key steps to arrive at the sequence-specific assignment are described below.

The sharp signals G′ and H′, which are geminal partners of G and H, show several strong connectivities. Signal G′ is dipole–dipole connected to four signals at 3.14, 2.93, 2.18, and 1.59 ppm, as shown in Figure 4B (cross peaks 1–4). The TOCSY experiment, shown in Figure 4C, identifies these signals as belonging to an Arg residue. Also, the NOESY cross peaks (not shown) are consistent with the assignment. There is a unique arginine in the primary sequence, at position 29, and such position is very close in space to Cys 8 (and far from all the other cysteine residues). In particular, Cys 8 $H\beta_2$ is expected to be, on the basis of the *P. aerogenes* ferredoxin structure,[89,90,93] at less than 2.4 Å from Arg 29 $H\beta_2$ and from Arg 29 $H\gamma_1$. On this basis, signals G and G′, originating from Cys VII (cluster I), can be assigned to Cys 8 $H\beta_1$ and $H\beta_2$, respectively. Signal H′ gives major cross peaks with signals at 4.14, 3.87 (cross peaks 5,6 Figure 4B), also observed from H but with smaller intensity, and 1.59 ppm (cross peak 7, Figure 4B). Signals at 4.11 and 1.59 ppm have strong NOESY and TOCSY connectivities typical of an Ala residue (Figure 4C). The signal at 3.87 ppm, which is dipole–dipole coupled to signal H′ (cross peak 6, Figure 4B) has also a NOESY and TOCSY pattern typical of an α-proton of an Ala residue (Figure 4C). Cys 37 $H\beta_2$ is very close in space to both αCH and βCH_3 of the Ala 1 residue and at least to the αCH of Ala 34. There are no other cysteine residues close to two Ala groups. This leads us to assign signal H′ (cysteine VIII, cluster II) as $H\beta_2$ of Cys 37 and its geminal partner as $H\beta_1$.

In the discussion of the pairwise assignment, we have already shown that Cys III and Cys IV can be sequence-specifically, stereospecifically assigned to Cys 14 and Cys 43 on the basis of the proximity between Hα of Cys 43 and $H\beta_1$ of Cys 14. A further evidence comes from the observation of connectivities with another signal at 0.54 ppm from both signals C and D (cross peaks 8 and 9, Figure 4A); this signal is assigned as the δCH_3 methyl resonance of Ile 23. Such a methyl group is also close to Cys 18. A weak NOE from signal F and Ile 23 δCH_3 is observed (cross peak 10 in Figure 4A). Signal F (Cys VI) is assigned to $H\beta_2$ of Cys 18. The $H\beta_1$ proton (signal F′) is still closer to Ile 23 δCH_3 but is too broad to allow the detection of any connectivity. As far as Cys I (cluster II) is concerned, signal A gives a strong cross peak with a signal at 1.01 ppm (cross peak 11 in Figure 4A), while no sizable connectivities are observed from A′. This is only consistent with the assignment of A as Cys 40 $H\beta_2$ and of A′ as Cys 40 $H\beta_1$, because, while in the structure of *P. aerogenes* ferredoxin Cys 39 $H\beta_2$ (corresponding to Cys 40) is at less than 2.5 Å from δCH_3 of Ile 37 (corresponding to Ile 38), Cys 39 $H\beta_1$ has no sizable contacts (*i.e.*, less than 3.0 Å) with any other proton. These assignments complete the assignment of cysteines coordinated to cluster II.

We are then left with the assignment of Cys 11 and 47, belonging to cluster I. The structural data show that, among the four βCH_2 protons of Cys 11 and Cys 47, Cys 47 $H\beta_2$ has the unique feature of being more than 3.0 Å apart form its αCH proton (already assigned through COSY), while there are three protons, *i.e.*, both δCH_2 of Pro 52 and the αCH of Asp 50 (replacing a Gly residue in the primary sequence of *P. aerogenes* ferredoxin), which are less than 3.0 Å apart from the Cys 47 $H\beta_2$. These three protons, as well as the αCH proton, are expected to fall in the 5–3-ppm region. Signal E is the only cysteine βCH_2 proton displaying a pattern of four cross peaks in that region (labeled 12–15 in Figure 4A), the weakest being already assigned to its αCH signal. This provides a strong evidence for the assignment of signal E as Cys 47 $H\beta_2$ and, as a consequence, of its geminal partner E′ as Cys 47 $H\beta_1$. Observations analogous to the case of Cys 40 hold also for Cys 11 (*i.e.*, the cysteine of cluster I closely corresponding to Cys 40 of cluster II, see below). Indeed, the occurrence of cross peaks between signal B and two resonances lying in the region of aliphatic signals leads us to assign signal B as Cys 11 $H\beta_2$, which is expected to be less than 3.0 Å apart from at least one CH_3 group (δCH_3 of Ile 9). Similarly to the case of Cys 40, its geminal partner does not give rise to any connectivity in such spectral region, consistent with the fact that it has no interresidue contacts at distances shorter than 4.0 Å. These findings provide the complete assignment of cluster-coordinated cysteines. The assignment is summarized in column 7 of Table 1. We note that, as previously observed for *C. pasteurianum* ferredoxin,[15,16,24] there is an almost perfect one-to-one correspondence between the proton signals of the two clusters. This correspondence indicates that the mirror symmetry apparent from X-ray data on *P. aerogenes* ferredoxin[89,90,93] is also maintained in the present case as it is in *C. pasteurianum* ferredoxin. In particular, very similar shifts and line widths are displayed by the protons of the following pairs from clusters I and II, respectively: Cys 8–Cys 37; Cys 11–Cys 40; Cys 14–Cys 43; Cys 47–Cys 18. We also note that this symmetry only breaks down when some NOESY connectivities of the βCH_2 signals with other diamagnetic signals are examined. Indeed, the two clusters are not surrounded by identical residues.

(93) Backes, G.; Mino, Y.; Loehr, T. M.; Meyer, T. E.; Cusanovich, M. A.; Sweeney, W. V.; Adman, E. T.; Sanders-Loehr, J. *J. Am. Chem. Soc.* **1991**, *113*, 2055.

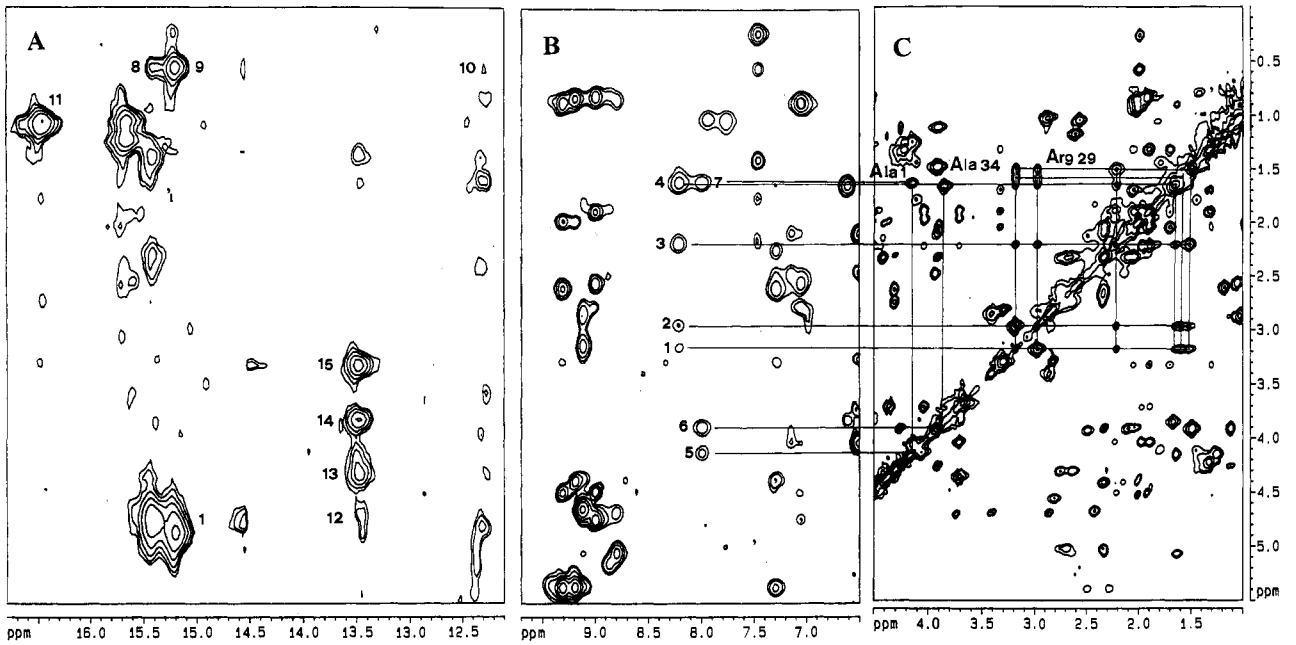

Figure 4. 600-MHz, 298 K NOESY (A and B) and TOCSY (C) experiments on fully oxidized ferredoxin from *C. acidi urici*. The regions of the NOESY and TOCSY maps which display the connectivities mentioned in the text and used to perform the sequence specific assignment of cysteines are shown. Cross peak assignments: (1) Cys 8 Hβ_2–Arg 29 Hδ, (2) Cys 8 Hβ_2–Arg 29 Hδ', (3) Cys 8 Hβ_2–Arg 29 Hβ_2, (4) Cys 8 Hβ_2–Arg 29 Hγ_1, (5) Cys 37 Hβ_2–Ala 1 Hα, (6) Cys 37 Hβ_2–Ala 34 Hα, (7) Cys 37 Hβ_2–Ala 1 βCH$_3$, (8) Cys 43 Hβ_1–Ile 23 δCH$_3$, (9) Cys 14 Hβ_1–Ile 23 δCH$_3$, (10) Cys 18 Hβ_2–Ile 23 δCH$_3$, (11) Cys 40 Hβ_2–Ile 37 δCH$_3$, (12) Cys 47 Hβ_2–Cys 47 Hα, (13–15) Cys 47 Hβ_2–Pro 52 δCH$_2$, Cys 47 Hβ_2–Asp 50 Hα. In the TOCSY map, the identified resonances of Arg 29, Ala 1, and Ala 34 are shown.

Comparison with the Ferredoxin from *C. pasteurianum*. The already published ^{1}H NMR spectra of the ferredoxin from *C. pasteurianum* are very similar to those obtained on the present system both in shifts and in line widths. The reported 2D NOESY spectra closely correspond to those of the present system. The TOCSY spectra for *C. pasteurianum* ferredoxin are not available, but the similarity of the NOESY maps reveals, in most cases, that the βCH$_2$ protons are dipolarly connected to the same type of residues.

The simple comparison of the geminal βCH$_2$ COSY connectivities of Figure 2A with those of oxidized *C. pasteurianum* ferredoxin[16,24] is sufficient to achieve the assignment reported in Table 1, columns 8–10. We note that the most relevant among the small differences between the spectra of the two oxidized proteins is the opposite hyperfine shift changes experienced by Cys 14 (Cys III) and Cys 43 (Cys IV) on passing from *C. pasteurianum* ferredoxin to *C. acidi urici* ferredoxin (the hyperfine shift change of Cys 43 causes its Hβ_1 signal (C) to be less shifted than the Hβ_2 signal of Cys 11 (B) in the present system). These modest differences in the hyperfine shifts of Cys 14 and Cys 43 in the two proteins may reflect the closer proximity of these two residues in *C. acidi urici* ferredoxin, as revealed by the sizable intercluster NOESY connectivity experienced by signal C.

^{13}C Spectra. HMQC experiments on oxidized ferredoxin from *C. acidi urici* has allowed us to observe ^{13}C–^{1}H scalar connectivities (Figure 5). Since all the βCH$_2$ protons have been assigned, it is possible to assign all the Cys β-carbons. The estimated ^{13}C hyperfine shifts and assignments are reported in Table 2. They have been obtained by subtracting from the observed chemical shift value the reported chemical shift values for Cβ and Cα cysteines bound to diamagnetic metal ions.[94] The ^{13}C hyperfine shifts range between 60 and 90 ppm. Six out of the eight Cα carbon signals have been also observed. Again, a close correspondence in the behavior of the two clusters is observed. The hyperfine shifts of the various carbon nuclei will be of help when analyzing the spin density transfer mechanisms. This is the first time that cysteine ^{13}C signals are observed at natural abundance in a Fe–S protein.

Table 2. Estimated Hyperfine Shifts of Protons and Carbons of Cluster-Coordinated Cysteines in Oxidized Ferredoxin from *C. acidi urici*[a] at 293 K and pH 7.8

cluster I				cluster II			
residue	atom	signal	δ (ppm)	residue	atom	signal	δ (ppm)
Cys 11	Hβ_1	B′	6.4	Cys 40	Hβ_1	A′	6.7
	Hβ_2	B	12.6		Hβ_2	A	13.5
	Cβ		66		Cβ		66
	Hα	B″	5.8		Hα	A″	5.5
	Cα		21		Cα		23
Cys 14	Hβ_1	D	12.2	Cys 43	Hβ_1	C	12.4
	Hβ_2	D′	2.0		Hβ_2	C′	2.0
	Cβ		90		Cβ		84
	Hα	D″	3.2		Hα	C″	2.2
	Cα		32		Cα		29
Cys 47	Hβ_1	E′	3.7	Cys 18	Hβ_1	F′	3.6
	Hβ_2	E	10.6		Hβ_2	F	9.4
	Cβ		78		Cβ		74
	Hα	E″	0.5		Hα	F″	0.8
	Cα				Cα		36
Cys 8	Hβ_1	G	8.6	Cys 37	Hβ_1	H	8.3
	Hβ_2	G′	5.4		Hβ_2	H′	5.1
	Cβ		60		Cβ		60
	Hα	G″	$\sim$0[b]		Hα	H″	$\sim$0[b]
	Cα				Cα		29

[a] Hyperfine shifts are estimated by subtracting from the experimental chemical shift values the following values: 2.8 ppm for Hβ protons, 4.2 ppm for Hα protons, 31 ppm for Cβ carbons, and 60 ppm for Cα carbons. These values have been chosen from reported chemical shifts of cysteines coordinated to zinc in zinc fingers (ref 94), as the closest models to our system. [b] The hyperfine shifts estimated by subtracting 4.2 ppm result slightly negative. These values are assumed to be zero within the indetermination of the reference shift.

Temperature Dependence of the Hyperfine Shifts in the Reduced Form. To understand the electronic structure of the reduced species, the establishment of the temperature dependence of the βCH$_2$ protons is required. This is experimentally difficult to achieve because of the above mentioned overlap among signals from the different species in solution. We have therefore decided

(94) Summers, M. F.; South, T. L.; Kim, B.; Hare, D. R. *Biochemistry* **1990**, *29*, 329.

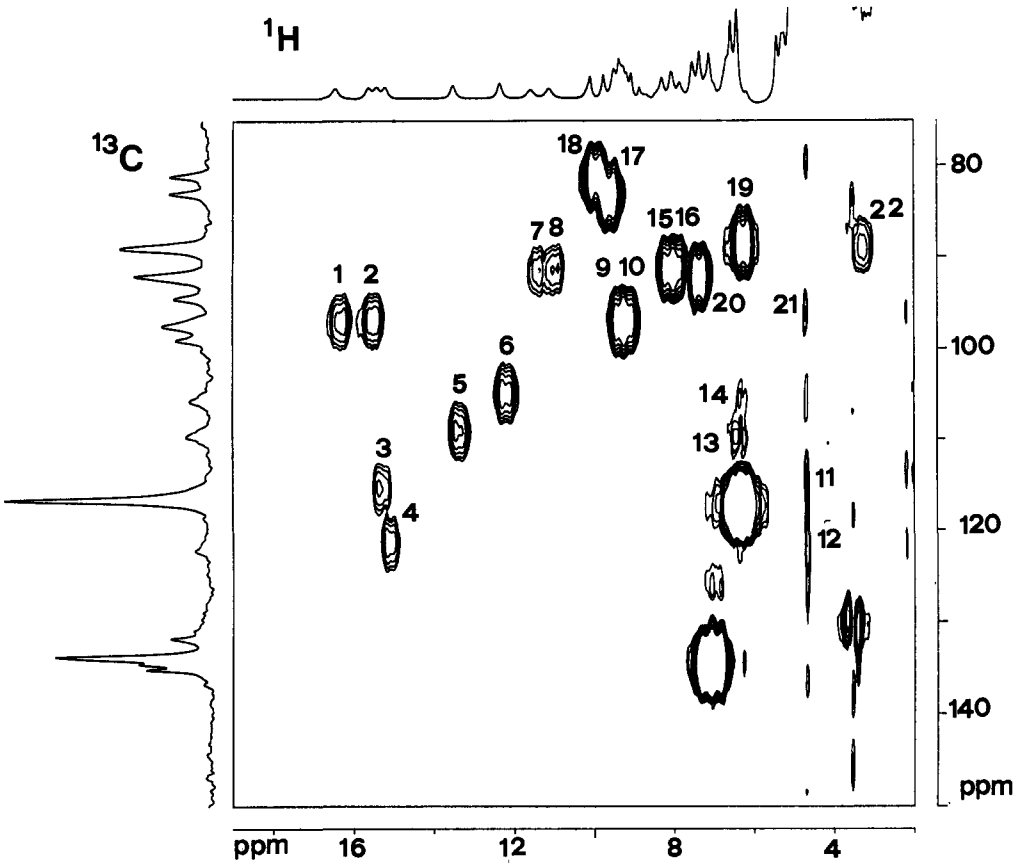

Figure 5. ^{13}C–^{1}H HMQC experiment recorded on oxidized ferredoxin from *C. acidi urici* at 298 K. The labeled cross peaks allows the detection of the ^{13}C resonances of the Cβ of the eight cluster-coordinated cysteines and six of the eight Cα resonances. Cross peak assignments: (1) Hβ_2–Cβ Cys 40, (2) Hβ_2–Cβ Cys 11, (3) Hβ_1–Cβ Cys 43, (4) Hβ_1–Cβ Cys 14, (5) Hβ_2–Cβ Cys 47, (6) Hβ_2–Cβ Cys 18, (7) Hβ_1–Cβ Cys 8, (8) Hβ_1–Cβ Cys 37, (9) Hβ_1–Cβ Cys 40, (10) Hβ_1–Cβ Cys 11, (11) Hβ_2–Cβ Cys 43, (12) Hβ_2–Cβ Cys 14, (13) Hβ_1–Cβ Cys 47, (14) Hβ_1–Cβ Cys 18, (15) Hβ_2–Cβ Cys 8, (16) Hβ_2–Cβ Cys 37, (17) Hα–Cα Cys 40, (18) Hα–Cα Cys 11, (19) Hα–Cα Cys 43, (20) Hα–Cα Cys 14, (21) Hα–Cα Cys 18, (22) Hα–Cα Cys 37. Conditions are reported in the Experimental Part.

to follow the temperature dependence of the EXSY cross peaks on partially reduced samples. The EXSY experiment reported in Figure 3 has been succesfully repeated at different temperatures, ranging from 282 to 300 K. Figure 6 shows the temperature dependencies of the signals of the reduced species, as obtained from the temperature dependencies of the relative cross peaks.

It appears that, for each cluster, two cysteine protons display a Curie behavior and two an anti-Curie behavior. For cluster I, Cys 8 and Cys 14 βCH_2 protons experience a Curie temperature dependence of the shifts, while Cys 47 and Cys 11 protons experience an anti-Curie temperature dependence. In the case of cluster II, Cys 43 and Cys 37 are of Curie type and Cys 18 and Cys 40 are of anti-Curie type (Table 1, column 11).

Angular Dependence of the Hyperfine Shifts. It is known that in metal–donor–CH_2 moieties of the type shown in Figure 7A there is a dependence of the hyperfine coupling on the dihedral angle θ formed by the M–D–C and D–C–H planes (Figure 7B). In the case of octahedral nickel(II) complexes with amine ligands, such dependence has been found to obey the general Karplus[72] relationship:

$$\delta = a' \cos^2 \theta + b' \cos \theta + c' \qquad (1)$$

where b' and c' are small and often neglected.[73-75] This equation originates from the nonorthogonality of the 1s orbitals of hydrogen atoms and the M–D σ bond, where spin density is present. If, however, the unpaired spin density sits on a pπ orbital of the D atom, the Karplus relationship becomes

$$\delta = a'' \sin^2 \theta + c'' \qquad (2)$$

where the $\sin^2 \theta$ dependence arises from the fact that the p orbital on the D atom is at 90° with respect to the M–D σ bond (Figure 7B). Equation 1 holds where, as in amine donors, no pπ orbitals are present. Equation 2 holds in organic sp^2 radicals, with the unpaired electron in the p_z orbital, θ being the angle between the sp^2 plane and the C–C–H plane.[95,96] When D is a cysteine sulfur, as in the present case, both mechanisms can be operative. Combining eqs 1 and 2, we obtain

$$\delta = a \sin^2 \theta + b \cos \theta + c \qquad (3)$$

where $a = a'' - a'$, $b = b'$, and $c = a' + c' + c''$. a is positive or negative depending on whether a'' is larger than a' or vice versa, *i.e.*, on whether the $\sin^2 \theta$ term in eq 2 dominates over the $\cos^2 \theta$ term in eq 1.

If we plot the hyperfine shifts of the βCH_2 protons of oxidized *C. acidi urici* ferredoxin versus the values of θ estimated from the X-ray structure of *P. aerogenes*[89,90,93] (Figure 8), a good fit of the data to eq 3 is obtained (solid line in Figure 8), with $a = 11.5$, $b = -2.9$, and $c = 3.7$ ppm. The large and positive a value indicates that the pπ mechanism of eq 2 is dominant, although the nonzero b value suggests that the σ mechanism of eq 1 may not be negligible.

Figure 8 reports, together with the hyperfine shifts of the cysteine βCH_2 protons of the present ferredoxin in the oxidized $[Fe_4S_4]^{2+}$ form (●), those of oxidized *C. pasteurianum* ferredoxin[15] (○) (of course referred to the same X-ray data) plus those of the βCH_2 protons of cysteines coordinated to the $[Fe_4S_4]^{2+}$ clusters of reduced *Cromatium vinosum* HiPIP[32] (△) and of reduced *Ectothirhodospira halophila* HiPIP II[35] (▽). The

(95) Heller, C.; McConnell, H. M. *J. Chem. Phys.* **1960**, *32*, 1535.
(96) Stone, E. W.; Maki, A. H. *J. Chem. Phys.* **1962**, *37*, 1326.

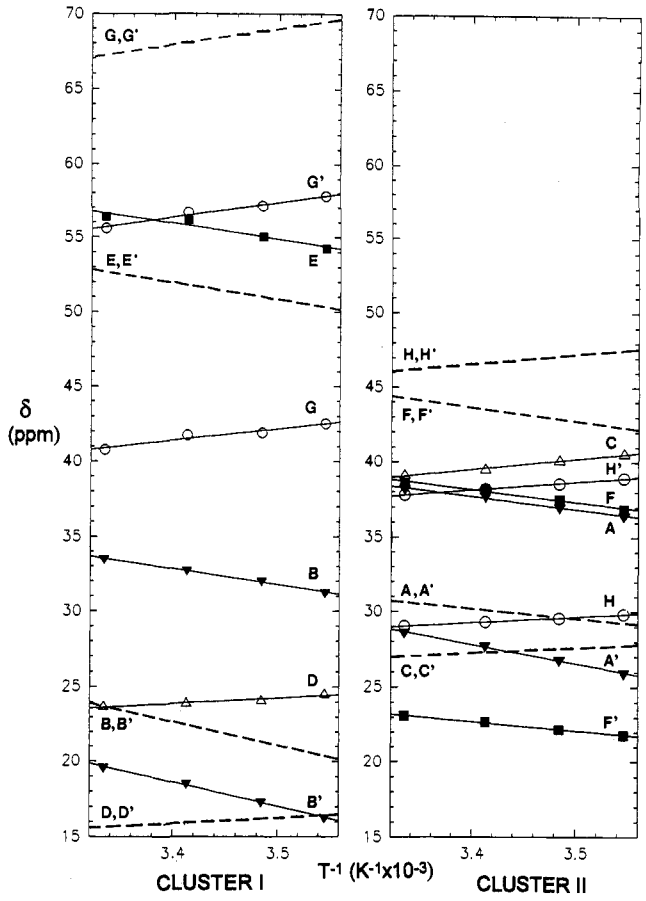

Figure 6. Experimental temperature dependence of chemical shifts of cysteine βCH_2 proton signals of fully reduced ferredoxin from *C. acidi urici* as obtained from EXSY experiments at different temperatures. The dashed lines represent estimates of the average angle-independent shifts for each βCH_2 pair (see text).

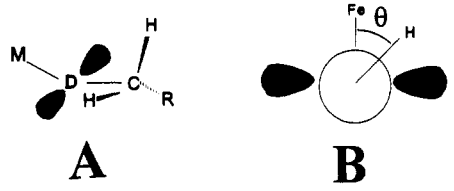

Figure 7. Schematic view of the M–D–C–H dihedral angle θ for metal donor CH_2 moieties. A p_z orbital of D orthogonal to the M–D–C plane is also shown.

dihedral angles of the former HiPIP are referred to X-ray data[97] and the latter to the MD-refined structure[35] starting from the X-ray structure of HiPIP I.[98] Furthermore, the hyperfine shifts of the six α-carbons assigned here (Table 2) can also be adjusted to the same behavior by a simple scaling down of the shifts (Figure 8). Although the solid line is the best-fit curve only for the shifts of the *C. acidi urici* cysteine βCH_2 protons (●), all other values are apparently in good agreement with the same functional form. This confirms that we are dealing with a general behavior and that the spin density transfer is essentially a $p\pi$ spin-transfer mechanism, as already qualitatively proposed by us.[33]

A result of this fitting is that the hyperfine coupling constants of the βCH_2 protons of all cysteines coordinating $[Fe_4S_4]^{2+}$ clusters are essentially equal and are only modulated by the dihedral angle. Furthermore, the hyperfine shifts of the α-carbons have the same angular dependence of the βCH_2 protons, although on a different scale. This is not surprising, since the α-carbons are geometrically similar to the βCH_2 protons. The result is that spin delocalization, even on the α-carbon, is more dictated by this angular dependence mechanism, which is also termed hyperconjugative mechanism, rather than through σ spin delocalization. The whole picture leads to the conclusion that the angle-independent part of the hyperfine coupling over the nuclei of the four cysteines is the same.[99]

The present finding of the angular dependence of the hyperfine coupling for many experimental data settles the debate[12,16,32,33,76,100] on the mechanism of spin density transfer in cysteine ligands and is enlightening with respect to the spin density transfer through any kind of donor atom.[73–75,95,96]

The problem arises of whether the same equation with similar parameters holds when one electron is added to or removed from the cluster (*i.e.*, for reduced ferredoxins and oxidized HiPIPs, respectively). In these cases, low-symmetry components are introduced which make one iron ion or two iron ions (in the case of two-center delocalization) inequivalent with respect to the other two. If this inequivalence can be theoretically handled, the further problem exists of different populations of d orbitals, which in principle provides different σ or π spin delocalization ratios. Nevertheless, if $\sin^2\theta$ or $\cos^2\theta$ terms prevail, by simply comparing the hyperfine shifts of geminal protons with the θ angle, the $\sin^2\theta$ or $\cos^2\theta$ dependence can be ascertained. The available data on oxidized HiPIP[32,35] and on a model complex[76,101] show a dominant $\sin^2\theta$ dependence, except when temperature-dependent conformational changes occur.[32,35] Also in the case of the present reduced ferredoxin, a $\sin^2\theta$ dependence is found to be dominant.

A Comment on the Electronic Structure of the $[Fe_4S_4]^+$ Cluster. The hyperfine shifts of each cysteine βCH_2 proton in both the oxidized and the reduced species are related to the electronic structure of the cluster through the hyperfine coupling constant. The angular-independent part of the latter, for simplicity and in agreement with the present findings, is taken to be equal for all iron ions. We are interested here in discussing the reduced species, which shows evidence of low-symmetry components. We note that all the hyperfine shifts are downfield and sizable. We then note that half of them have a Curie and half of them an anti-Curie temperature dependence. This shows that the iron ions are at least pairwise inequivalent. In all the other cases in which Curie and anti-Curie behaviors are observed (*i.e.*, oxidized HiPIPs[31–35] and reduced $Fe_2S_2^+$ cores[102,103]), the shifts of Curie type are much larger than the others. In some cases, upfield and downfield shifts have been observed. This was accounted for on the basis of a simplified model in which a larger subspin (associated with one or two iron ions depending on the system) determines the large downfield shifts and the Curie behavior and a smaller subspin determines the anti-Curie behavior and the upfield shifts.

In an attempt to understand the experimental behavior, we have corrected the proton hyperfine shifts for the different θ angles by assuming that eq 3 holds for $[Fe_4S_4]^+$ clusters and that the θ angles are the same in both reduced and oxidized species. To do so, we have simply divided the hyperfine shift value of each signal in the reduced species by the hyperfine shift value in the oxidized species and multiplied the result by the average value of eq 3 calculated from the best-fit parameters of the oxidized form ($\delta_{av} = a/2 + c$). In this way we have rendered the shifts "angle independent". The result is that (dashed lines in Figure 6) there are two signals of both Curie and anti-Curie type far shifted and two, again of both Curie and anti-Curie type, less

(97) Carter, C. W. J.; Kraut, J.; Freer, S. T.; Alden, R. A. *J. Biol. Chem.* **1974**, *249*, 6339.
(98) Breiter, D. R.; Meyer, T. E.; Rayment, I.; Holden, H. M. *J. Biol. Chem.* **1991**, *266*, 18660.
(99) The β-carbons have significantly different shifts (75 ± 15 ppm). Since the contributions to the β-carbon shifts may be several, in this case the inequivalence among the β-carbon atoms seems to be magnified.
(100) Nettesheim, D. G.; Harder, S. R.; Feinberg, B. A.; Otvos, J. D. *Biochemistry* **1992**, *31*, 1234.
(101) Actually, the authors of ref 76 have used a different functional form. However, their data well fit our eq 3 with a very small cos θ term.
(102) Dunham, W. R.; Palmer, G.; Sands, R. H.; Bearden, A. J. *Biochim. Biophys. Acta* **1971**, *253*, 373.
(103) Banci, L.; Bertini, I.; Luchinat, C. *Struct. Bonding* **1990**, *72*, 113.

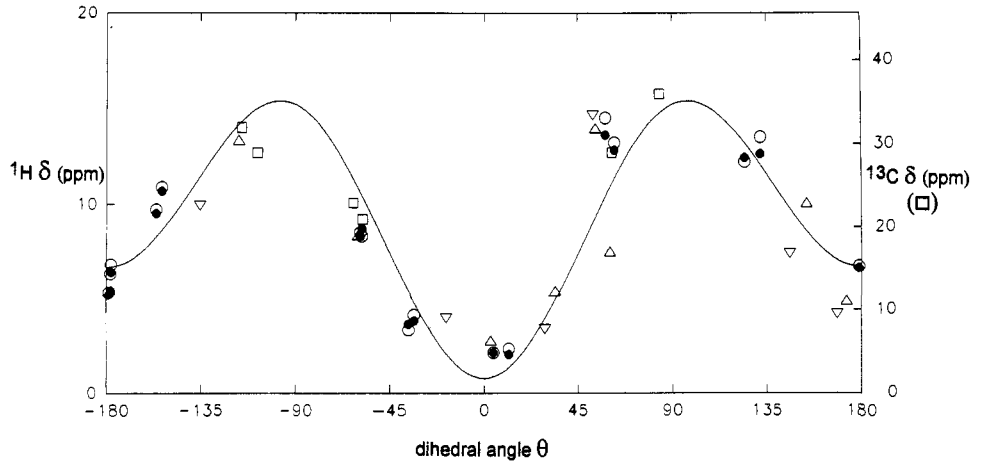

Figure 8. Plot of the hyperfine shifts of cysteine βCH_2 protons, (left-hand scale) and Cα carbons (□) (right-hand scale) for some proteins containing $[Fe_4S_4]^{2+}$ clusters as a function of the dihedral angles θ, Fe–S–Cβ–H and Fe–S–Cβ–Cα, respectively. The hyperfine shifts of βCH_2 protons from different proteins are reported as follows: (●) oxidized *C. acidi urici* ferredoxin, (○) oxidized *C. pasteurianum* ferredoxin,[15] (△) reduced *C. vinosum* HiPIP,[32] (▽) reduced *E. halophila* HiPIP II.[35] The curve reports the fitting of the 16 values of *C. acidi urici* ferredoxin (●) on the basis of eq 3. The best-fit values obtained for the three parameters are a = 11.5, b = −2.9, and c = 3.7 ppm.

shifted for each cluster. Similar conclusions can be reached for *C. pasteurianum* ferredoxin. Note that the anti-Curie behavior in the case of *C. pasteurianum* ferredoxin is less marked than in the present system.[24]

All of these properties are at the moment not understood in detail. We can, however, say that they point toward a $[Fe_4S_4]^+$ core in which the antiferromagnetic coupling constants J for each bimetallic center are smaller than in the case of oxidized HiPIPs. If J were $\ll kT$, all the shifts would have been equal (besides the difference in $S(S+1)$ for the various ions) and downfield.

It has been pointed out in several occasions that in the case of mixed-valence systems the effective J value is reduced by electron delocalization.[78,79,104,105] A possibility is, therefore, that electron delocalization makes the iron ions more similar to each other than in the case of HiPIPs. Mössbauer spectra which do not resolve the various iron ions seem to be in agreement with this observation. Small J values are in accord with $S = {}^3/_2$ or ${}^7/_2$ being close to the ground state and sometimes becoming the ground state in model systems[106,107] or when Se substitutes S.[108,109] In the framework of a Heisenberg Hamiltonian of the type

$$\mathcal{H} = \sum_{i \neq j} J_{ij} S_i \cdot S_j \qquad (4)$$

and following well known procedures, J_{ij} values of the order of 100 cm^{-1} would give the right extent of the hyperfine shifts; as already noted,[24] small differences among J_{ij} values would give a variety of temperature dependencies.

As far as other reduced ferredoxins are concerned, the lack of sequence-specific assignments prevents the estimate of angle-independent shifts in the reduced forms. As far as one can judge from the hyperfine shifts as such, in three one-cluster proteins from *B. polymixa*,[26] *B. thermoproteolyticus*,[25] *and B. stearothermophilus*,[25] the average of all shifts with Curie temperature dependence is higher than the average of all shifts with anti-Curie temperature dependence. Interestingly, Mössbauer data on reduced ferredoxin from *B. stearothermophilus*[9-11] show a slight inequivalence between the two pairs at zero field, although much smaller than that observed in oxidized HiPIPs. Magnetic Mössbauer data then show that the pair with the larger isomer shift (more ferrous) has a smaller subspin than the pair with the smaller isomer shift (more oxidized iron ion).[9] This would indicate a slightly larger inequivalence of the iron ions, still fitting in the above general frame. More independent experimental data are needed to characterize these systems.

Acknowledgment. Thanks are expressed to Dr. S. Tilli and Dr. V. Mignoni for the help in the biochemical work. A.V. acknowledges the International Center for Genetic Engineering and Biotechnology (UNIDO) for a fellowship and Fundacion Antorchas for further support. This work was supported by C.N.R., Progetto Finalizzato Biotecnologie e Biostrumentazione.

(104) Papaefthymiou, V.; Girerd, J.-J.; Moura, I.; Moura, J. J. G.; Munck, E. *J. Am. Chem. Soc.* **1987**, *109*, 4703.
(105) Bertini, I.; Briganti, F.; Luchinat, C. *Inorg. Chim. Acta* **1990**, *175*, 9.
(106) Noodleman, L. *Inorg. Chem.* **1991**, *30*, 246.
(107) Carney, M. J.; Papaefthymiou, G. C.; Spartalian, K.; Frankel, R. B.; Holm, R. H. *J. Am. Chem. Soc.* **1988**, *110*, 6084.
(108) Moulis, J.-M.; Auric, P.; Gaillard, J.; Meyer, J. *J. Biol. Chem.* **1984**, *259*, 11396.
(109) Gaillard, J.; Moulis, J.-M.; Auric, P.; Meyer, J. *Biochemistry* **1986**, *25*, 464.